diversity

MDPI

Article

Spatiotemporal Assessment of Water Quality, Phytoplankton Diversity, and Biometric Indicators in Aquaculture During a Marine Mucilage Event

Mustafa Tolga Tolon [1] and Levent Yurga [2,*]

[1] Department of Aquaculture, Faculty of Fisheries, Ege University, Bornova, İzmir 35040, Türkiye; tolga.tolon@ege.edu.tr
[2] Department of Marine–Inland Waters Sciences and Technology, Faculty of Fisheries, Ege University, Bornova, İzmir 35040, Türkiye
* Correspondence: levent.yurga@ege.edu.tr

Abstract

Marine mucilage events are intensifying in semi-enclosed seas under accelerating climate- and nutrient-driven pressures, yet their ecosystem-level consequences for aquaculture-linked coastal habitats remain insufficiently documented. This study provides an integrated spatiotemporal assessment of water quality, phytoplankton community structure, and biometric responses of *Mytilus galloprovincialis* during and after the 2025 mucilage outbreak in the Gulf of Erdek (Sea of Marmara, Türkiye). Mucilage accumulation was associated with sharp increases in turbidity, total suspended solids, and particulate organic matter, alongside declines in dissolved oxygen and pH. Phytoplankton assemblages exhibited marked seasonal restructuring: the mucilage period was characterized by the coexistence of mucilage-forming taxa, non-toxic bloom-forming species, and multiple harmful algal bloom (HAB) groups, including DSP- and ASP-related species, whereas post-mucilage conditions were dominated by non-toxic diatoms with substantially reduced HAB representation. The dinoflagellate species representing the May period in terms of abundance were *Noctiluca scintillans* and *Prorocentrum micans*; the diatom species were *Chaetoceros radiatus*, *Cylindrotheca closterium*, *Pseudo-nitzschia pseudodelicatissima*, and *Thalassiosira rotula*; and the coccolithophore was *Phaeocystis pouchetii*. Mussel biometric analyses revealed biometric indices and condition values markedly below regional historical baselines during the mucilage event, alongside reduced meat yield, followed by pronounced compensatory growth during the post-mucilage period. Our findings demonstrate that mucilage acts as both a physical and biological stressor, driving short-term ecological shifts in phytoplankton diversity and imposing substantial but reversible physiological impacts on mussel stocks. These results underscore the need for continuous biodiversity monitoring frameworks that integrate mucilage dynamics, HAB occurrence, and aquaculture resilience in regions vulnerable to climate-enhanced organic aggregate formation.

Keywords: biodiversity; environmental stressors; coastal ecosystem resilience; Sea of Marmara; harmful algal blooms (HAB); marine mucilage; *Mytilus galloprovincialis*; condition index

Check for updates

Academic Editors: Roberto Sandulli, Zhangxi Hu and Yunyan Deng

Received: 9 March 2026
Revised: 9 April 2026
Accepted: 16 April 2026
Published: 21 April 2026

Copyright: © 2026 by the authors. Licensee MDPI, Basel, Switzerland. This article is an open access article distributed under the terms and conditions of the Creative Commons Attribution (CC BY) license.

1. Introduction

Marine mucilage is a gelatinous, sticky organic aggregate formed by the excessive production of exopolymeric substances (EPS), composed of polysaccharides, proteins, lipids,

and other organic and inorganic particles, primarily by phytoplankton and bacteria under stress conditions such as nutrient enrichment, rising sea temperatures, and water column stratification [1], manifesting as cloudy water, floating flocs, or dense surface scums. Although mucilage events in the Adriatic Sea have been documented since at least 1729 [2,3], systematic scientific investigation intensified only following the large-scale outbreaks of the late 1980s and 1990s. Since then, the frequency, spatial extent, and persistence of mucilage have markedly increased, particularly in semi-enclosed seas such as the Mediterranean, where prolonged water residence time [4], thermally driven stratification [5], and riverine nutrient loading [6] collectively create conditions conducive to large-scale aggregation, rendering these events important indicators of ecosystem degradation driven by eutrophication, climate change, and anthropogenic pollution.

The Sea of Marmara, a semi-enclosed basin situated between the Aegean and Black Seas, has emerged as a critical hotspot for marine mucilage events. Mucilage was first officially reported along the northeastern coast of the Sea of Marmara, particularly off the shores of İzmit and Erdek (Balıkesir, Türkiye), in October 2007 [7]. Further occurrences were observed in 2010 along the coasts of Erdek and Büyükada (İstanbul) [8] and a significant mucilage outbreak covering the entire Sea of Marmara in autumn 2021 resulted in a major environmental disaster [9], extending into the Aegean Sea via the Dardanelles Strait and persisting until year's end. Subsequently, mucilage remained on the seabed in the coastal areas of the Sea of Marmara, specifically in the Gulf of Erdek, throughout 2023 and 2024 [10], and resurfaced in 2025, posing ongoing risks to the region's ecological balance.

The Sea of Marmara is of substantial economic and ecological importance as a primary site for the aquaculture of Mediterranean mussels (*Mytilus galloprovincialis* Lamarck, 1819) in Türkiye. With 39 mussel farms located on the shores of Balıkesir (16 farms), Bursa (9 farms), Yalova (7 farms) and Çanakkale (7 farms), the region produced 8085 metric tons in 2024, representing approximately 71.42% of Türkiye's total Mediterranean mussel aquaculture output [11]. Despite this economic significance, recurring marine mucilage events since 2007 have imposed severe ecological and economic consequences on these operations [12–15]. Dense gelatinous aggregates cover mussel beds and aquaculture infrastructure, generating hypoxic or anoxic conditions that impair mussel survival and growth [16–18], disrupt filter feeding and respiration, and promote the proliferation of pathogenic microorganisms [19]. Environmental conditions associated with mucilage formation further alter nutrient availability and particulate organic matter (POM) dynamics, with cascading negative effects on bivalve health, growth, and productivity [20]. Together, these stressors pose a serious threat to the sustainability and economic viability of aquaculture in mucilage-prone regions [1,21,22].

Yet despite the documented scale of these disruptions, quantitative assessments of mucilage impacts on aquaculture production outputs, including physiological and biometric effects on cultured organisms, remain conspicuously absent from the literature. It is also unclear how water quality and phytoplankton community dynamics during mucilage events interact to determine mussel growth responses, or whether recovery trajectories differ between acute outbreak and post-event periods. This represents a critical knowledge gap that constrains evidence-based management and policy responses, particularly as climate change amplifies the frequency and severity of mucilage events [23,24], and monitoring frameworks become increasingly important [25].

To address these gaps, this study investigated the causal relationships between water quality, phytoplankton composition, and mussel growth parameters during and after a mucilage event in 2025 at Mediterranean mussel aquaculture facilities in the Sea of Marmara. We tested three hypotheses: (i) mucilage accumulation significantly depresses mussel growth and condition indices relative to post-event recovery periods; (ii) water

quality deterioration during mucilage, specifically hypoxia and elevated organic loading, mediates the observed effects on mussel physiology; and (iii) shifts in phytoplankton community composition toward HAB species and mucilage-forming taxa reduce food quality and quantity available to filter feeders, compounding the direct physical impacts of aggregate accumulation.

The ecological and economic dimensions of mucilage are well established at broader scales. During the 2007–2008 Sea of Marmara outbreak, catch reductions for pelagic species reached 99.4% for anchovy and 93.4% for mackerel, with individual fishermen sustaining average annual income losses of €27,459, a 61.4% revenue decline, alongside sunk costs averaging €14,123 per vessel [26,27]. The 2021 event paralyzed marine operations for up to six months, with small-scale operators reporting 50–80% reductions in catch efficiency and industrial purse seine vessels experiencing near-total income losses of up to €400,000 per vessel [26,27]. Mucilage has also been documented to clog nets, pipelines, water intake and filtration systems, and shellfish farming equipment, collectively impeding water exchange and elevating mortality among cultured organisms [23,28–30]. The mucilage matrix further acts as a concentrated reservoir for pathogens including *Vibrio harveyi*, *V. parahaemolyticus*, *V. cholerae*, *Escherichia coli* O157:H7, *Salmonella* spp., *Listeria monocytogenes*, *Aeromonas hydrophila*, *Clostridium perfringens*, and *Bacillus cereus*, posing infectious risks to farmed organisms and human consumers alike [23,31]. Furthermore, the proliferation of harmful bacteria associated with mucilage poses risks to consumer health, negatively impacting consumer confidence and the marketability of mussels [9,31]. Notable mucilage events have also been documented elsewhere, including the North Sea in 1977 [32], Tasman Bay, New Zealand, in 1981 [33], the Adriatic Sea in 1988 [18,34], the Tyrrhenian Sea in 1991 [35], the Ligurian Sea in 2003 [29], and the northern Aegean Sea in 2008 [36], underscoring the global relevance of this phenomenon.

2. Materials and Methods

This study was conducted in the Gulf of Erdek (Balıkesir, Marmara Sea, Türkiye), where mussel farming activities are concentrated. The Gulf of Erdek is a semi-enclosed shallow embayment located along the southwestern coast of the Sea of Marmara, situated to the west of the Kapıdağ Peninsula and sheltered by the Marmara Islands archipelago to the north. The Sea of Marmara itself is a semi-enclosed basin of roughly 11,350 km^2, with depth transitioning from a shallow, gently sloping shelf along its southern boundary to steep bathymetry near its northern edge, encompassing three deep interior depressions. The Gulf of Erdek is characteristic of the southern shelf zone, with relatively shallow depths generally not exceeding 30–40 m, a predominantly muddy to sandy sediment composition, and the presence of *Posidonia oceanica* and other benthic habitats that support both wild populations and aquaculture operations, including longline mussel farming.

Water quality parameters, phytoplankton composition, and biometric characteristics of mussels at two aquaculture sites were examined during two contrasting periods: the mucilage event in May 2025 and the post-mucilage period in October 2025. Aquaculture station M1 was located approximately 125 m offshore at Ocaklar village on the northern shoreline of the Gulf of Erdek (40°27′42.59″ N, 27°42′33.17″ E), while station M2 was situated approximately 150 m offshore at Edincik village on the southern shoreline (40°19′42.76″ N, 27°47′43.75″ E). The two stations were separated by approximately 17 km along a north–south transect. A reference station (R) was established in the central part of the Gulf of Erdek, approximately 3000 m from shore and 7500 m from the mussel farms (40°23′6.19″ N, 27°45′16.85″ E), to characterize ambient open-water conditions within the gulf and to provide a baseline against which nearshore water quality at the aquaculture

stations could be compared; it was not intended to replicate the hydrographic or biological conditions of the coastal farm sites (Figure 1).

Figure 1. Locations of sampling stations in Mediterranean mussel aquaculture facilities: M1, Ocaklar (40°27′42.59″ N, 27°42′33.17″ E); M2, Edincik (40°19′42.76″ N, 27°47′43.75″ E). The reference station (R) is located 3 km off the coast of the Erdek District (40°23′6.19″ N, 27°45′16.85″ E) in the Gulf of Erdek, Sea of Marmara, Türkiye.

Water quality parameters were measured using calibrated portable field instruments. Dissolved oxygen was measured with a Milwaukee MW600 (Milwaukee Instruments, Inc., Rocky Mount, NC, USA) polarographic meter (resolution: 0.1 mg L^{-1}; accuracy: ±1.5% full scale), salinity and temperature with a Hanna HI98319 (Hanna Instruments Inc., Woonsocket, RI, USA) conductivity-based tester (resolution: 0.1 ppt and 0.1 °C; accuracy: ±1 ppt and ±0.5 °C, respectively), pH with an XS Instruments PC5 (Giorgio Bormac S.r.L., Carpi, Modena, Italy) multiparameter tester (resolution: 0.01 pH; accuracy: ±0.01 pH), and

turbidity with a WTW Turb 355 (WTW, Weilheim, Germany) nephelometric turbidimeter (resolution: 0.1 NTU in the 10–99.9 NTU range; accuracy: ±2% of measured value up to 500 NTU), compliant with US EPA 180.1 standards. The measurements were performed by sensor probes or water samples in triplicate at the depth of approximately 5 m below the surface where the dense mucilage is aggregated. Seawater samples from the stations M1, M2, and R were also collected using pre-cleaned 1000 mL polyethylene bottles and transported to laboratories at the Ege University, Faculty of Fisheries, İzmir (Türkiye) in dark containers maintained at +4 °C to minimize biological degradation.

Total suspended solids (TSS), particulate organic matter (POM), and particulate inorganic matter (PIM) in water samples were determined using the standard gravimetric method. A known volume (500 to 1000 mL) of mucilage-containing seawater samples was adjusted to the clogging limit of pre-combusted (450 °C, 4 h) Whatman GF/F glass fiber filters (0.7 µm pore size) and filtered under vacuum. The filters were rinsed with distilled water to remove residual salts, dried at 105 °C to a constant weight, and reweighed to the nearest 0.001 g using an analytical balance (OHAUS PR523, OHAUS Europe GmbH, Nänikon, Switzerland). TSS concentration was determined by subtracting the initial filter weight from the final filter weight and normalizing the result to the volume of water filtered. Measurements were performed in triplicate to ensure accuracy.

POM was determined using the loss-on-ignition method [37] by combusting dried glass fiber filters from TSS analysis at 450 °C for 4 h and reweighing to determine the organic fraction, which primarily consists of mucilage polysaccharides and cellular debris. Weight loss during ignition represents POM, whereas the residue remaining on the filter after ignition represents the inorganic or mineral fraction, PIM. POM and PIM concentrations were expressed as mg L^{-1}. The proportional representation of the organic load at the sampled stations was determined using the following equation:

$$Organic\ Matter\ Ratio(\%) = \mathrm{POM/TSS} \quad (1)$$

Seawater samples containing phytoplankton were collected from stations M1 and M2 using pre-cleaned 5 L polyethylene bottles from 0.5–1 m below the surface. The samples were fixed with 4% formaldehyde and transported on the same day to laboratories at the Faculty of Fisheries, Ege University, İzmir (Türkiye) in insulated containers maintained at +4 °C. Subsequently, the seawater was transferred into glass tubes and labeled according to the sampling stations using a two-step sedimentation procedure [38]. Species identification was conducted using the single-drop method [39] under an Olympus BX43 phase-contrast microscope. Taxonomic identification of diatom and dinoflagellate species was carried out with reference to the following standard works: Anderson [40], Balech [41], Cupp [42], Delgado and Fortuño [43], Dodge and Hart-Jones [44], Hasle and Syvertsen [45], Hendey [46], Koray et al. [47], Lebour [48], Marshall [49], Rampi and Bernhard [50], Rampi and Bernhard [51], Johansen [52], Steidinger and Tangen [53], Steidinger and Williams [54], Sournia [55], Sournia [56], Sournia [57], Taylor [58], Tomas [59], Trégouboff and Rose [60], and Wood [61]. Ciliophora species were identified in accordance with Boltovskoy [62], Isamu [63], Lee and Kim [64], Margalef [65], and Pierce and Turner [66]. Current nomenclature was verified using AlgaeBase [67] and WoRMS [68]. The phytoplankton samples were examined for the presence, spatial, and temporal distribution of harmful algal bloom (HAB) taxa, including dinoflagellate species associated with Paralytic Shellfish Poisoning (PSP), Diarrhetic Shellfish Poisoning (DSP), Neurotoxic Shellfish Poisoning (NSP), and diatom species responsible for Amnesic Shellfish Poisoning (ASP), as well as mucilage-forming (MU), non-toxic blooming species (NT), and toxic species (T). HAB taxa were determined using the methods described by Hallegraeff et al. [69] and Landsberg [70].

The biometric parameters of mussels were examined using 50 samples collected from each aquaculture station (M1 and M2) at sampling period. *M. galloprovincialis* were collected using a stratified random sampling protocol, whereby approximately 10 individuals were randomly selected from each of five independent longlines to ensure spatial independence of replicates and avoid pseudoreplication [71]. Sampled individuals were selected randomly along the top 5 m of each rope where the dense mucilage aggregates accumulated. Mussel samples from May 2025 were grouped as M1MUS and M2MUS for stations M1 and M2, respectively. Similarly, mussels sampled in October 2025 were grouped as M1REC and M2REC for stations M1 and M2, respectively. The sampled mussels were placed in labeled sample bags without fixation upon collection and transported to the laboratory in cooler boxes at +4 °C. External fouling organisms were removed prior to biometric measurements. The total shell length (TL), total shell width (TW), and total shell height (TH) were measured using a digital caliper to the nearest 0.01 mm. The adductor muscles were severed to isolate the soft tissues from the shells. Both soft tissue and shell samples were weighed to the nearest 0.001 g and subsequently dried in an oven at 80 °C until a constant weight was achieved. The condition index (CI) is one of the most practical and reliable growth indicator metrics used in mussel biology, aquaculture, and environmental monitoring, and provides a powerful means to assess the health, growth, and physiological status of mussels. The CI was calculated according to Crosby [72]:

$$\mathrm{CI} = \frac{\textit{Dry meat weight (g)}}{\textit{Dry shell weight (g)}} \times 100 \quad (2)$$

All environmental variables were tested for normality using the Shapiro–Wilk test and for homogeneity of variances using Levene's test prior to inferential analyses. Data were log-transformed as necessary to meet the assumptions of parametric testing. A two-way analysis of variance (ANOVA) was applied to evaluate the effects of sampling period (May 2025, mucilage period; October 2025, post-mucilage period) and station (M1, M2, R) and interaction (Period × Station) on each measured parameter. Significant main effects or interactions ($p < 0.05$) were followed by post hoc comparisons using Tukey's HSD test to identify pairwise differences among groups. The Kruskal–Wallis test, followed by Dunn–Bonferroni post hoc comparisons, was used to evaluate data obtained from mussel biometric measurements, including total shell length, total shell weight, total shell height, dry shell weight, dry meat weight, and condition index. The selection of parametric versus non-parametric procedures was determined by the outcome of normality and homogeneity tests applied independently to each variable, irrespective of the sampling design structure. Results are presented as means ± standard deviation. All statistical analyses were conducted using IBM SPSS v.27, with a significance level of $p < 0.05$.

3. Results

Marine mucilage formations were detected at all sampled stations during sampling conducted via scuba diving in May 2025, forming stratified layers extending from the seabed (approximately 30 m) to the surface. Mucilage aggregates in the bottom and midwater layers exhibited slow northward movement. At the seabed, thick, cloud-like mucilage formations appeared in shades of light yellow and white (Figure 2a). Mussel longlines were covered with dense mucilage aggregates up to a depth of approximately 10 m below the surface (Figure 2b), and mussels were sparsely attached to the ropes (Figure 2c). The attachment strength of the mussels to the cultivation ropes was rather low, and they were easily detached from the ropes (Figure 2d).

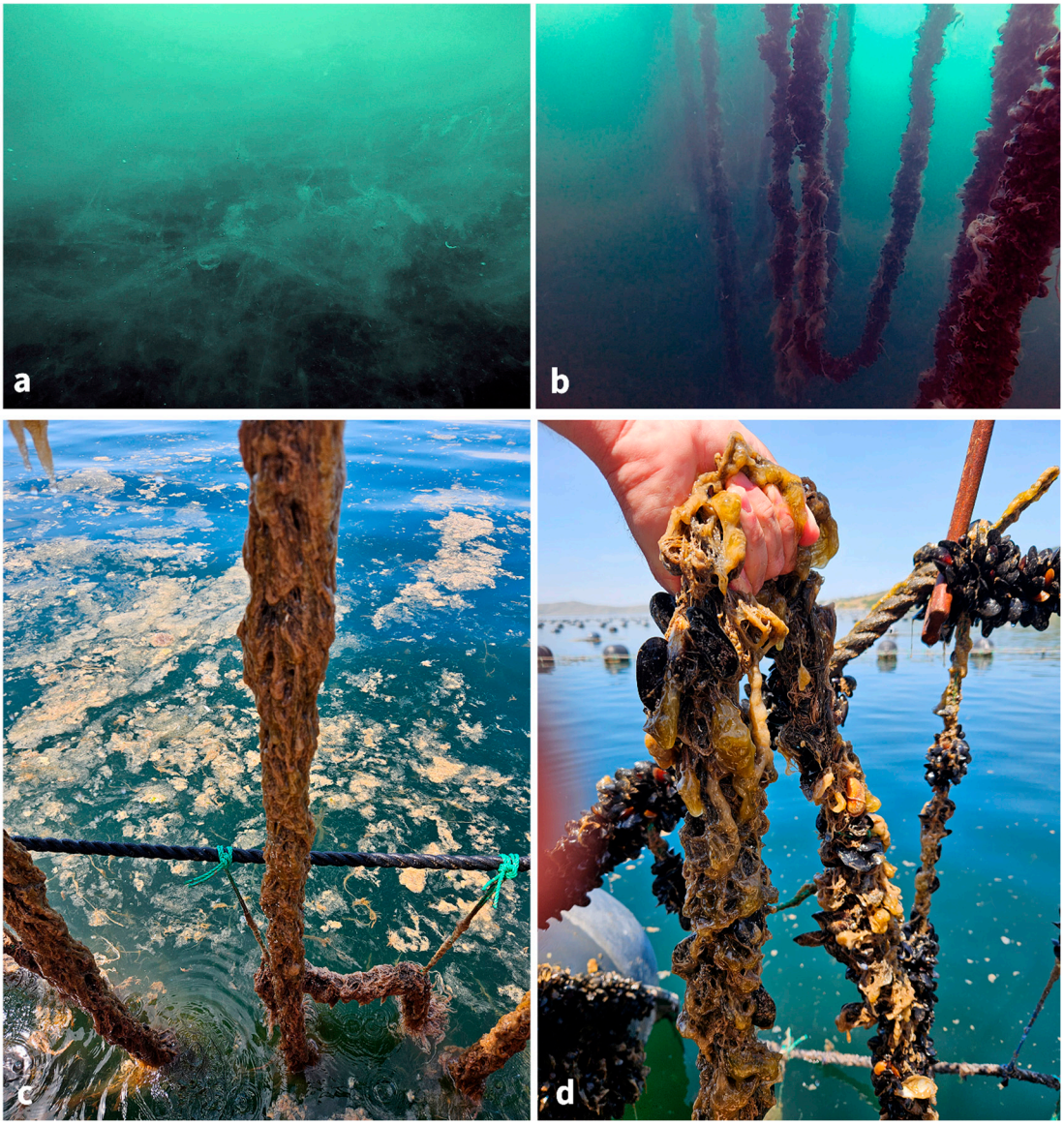

Figure 2. (**a**) Cloud-like dense mucilage layers rapidly dispersing at the seabed; (**b**) Mussel longlines covered with dense mucilage aggregates; (**c**) Mucilage-covered and sparsely attached mussels on cultivation ropes; (**d**) Ease of mussel detachment from the ropes at M1 and M2 stations in May 2025, Gulf of Erdek (Sea of Marmara, Türkiye).

Two-way ANOVA revealed a strong effect of sampling period on most environmental parameters; station effects were parameter-specific and most pronounced during the mucilage period, particularly for dissolved oxygen, pH, turbidity, TSS, and POM, whereas spatial differences were negligible for temperature, salinity, and particulate inorganic matter. No significant station effect or Period × Station interaction was detected for either water temperature or salinity variables ($p > 0.05$). Dissolved oxygen was significantly affected by both period and station ($p < 0.05$), with markedly higher concentrations observed in October compared with May, and the highest values consistently recorded at reference station R. However, no significant interaction was detected ($p > 0.05$). Similarly, pH showed significant main effects of both period and station ($p < 0.05$), with higher values recorded during the post-mucilage period and the highest values observed at station M2, while the Period × Station interaction remained non-significant (Table 1).

Table 1. Environmental parameters (mean ± SD) measured at two stations and at a reference station (M1, M2, and R) during May 2025 (mucilage event) and October 2025 (post-mucilage period). Superscript letters in each row denote significance across both spatial and temporal dimensions for the related parameters ($p < 0.05$).

Parameter	Unit	May 2025 (Mucilage)			October 2025 (Post-Mucilage)		
		M1	M2	R	M1	M2	R
Temperature	°C	22.5 ± 0.2 ^{a}	22.1 ± 0.1 ^{a}	21.8 ± 0.3 ^{a}	19.0 ± 0.9 ^{a}	19.0 ± 1.0 ^{a}	20.9 ± 0.2 ^{a}
Salinity	ppt	27.1 ± 0.7 ^{a}	26.4 ± 0.4 ^{a}	26.8 ± 0.8 ^{a}	24.8 ± 0.1 ^{a}	24.9 ± 0.1 ^{a}	25.1 ± 0.5 ^{a}
Dissolved oxygen	mg L^{-1}	3.1 ± 0.4 ^{a}	3.8 ± 0.2 ^{a}	4.4 ± 0.2 ^{ab}	6.5 ± 0.4 ^{b}	5.8 ± 0.2 ^{b}	7.5 ± 0.2 ^{c}
pH	-	7.02 ± 0.11 ^{a}	6.67 ± 0.14 ^{a}	7.07 ± 0.11 ^{a}	7.43 ± 0.23 ^{ab}	7.89 ± 0.03 ^{b}	7.30 ± 0.07 ^{ab}
Turbidity	NTU	51.06 ± 3.12 ^{a}	53.35 ± 3.84 ^{a}	41.87 ± 2.74 ^{b}	6.34 ± 0.36 ^{c}	7.13 ± 0.28 ^{c}	7.86 ± 0.11 ^{c}
TSS	mg L^{-1}	82.7 ± 2.9 ^{a}	89.4 ± 3.2 ^{a}	77.1 ± 2.1 ^{b}	7.1 ± 0.9 ^{c}	7.6 ± 1.2 ^{c}	7.2 ± 0.9 ^{c}
POM	mg L^{-1}	56.2 ± 1.2 ^{a}	64.5 ± 2.3 ^{a}	47.3 ± 1.1 ^{b}	4.4 ± 0.2 ^{c}	4.5 ± 0.4 ^{c}	3.9 ± 0.7 ^{c}
PIM	mg L^{-1}	26.5 ± 3.1 ^{a}	24.9 ± 3.9 ^{a}	29.8 ± 2.4 ^{a}	2.7 ± 0.9 ^{b}	3.1 ± 1.3 ^{b}	3.3 ± 1.1 ^{b}
OMR	%	68	72	61	62	59	54

TSS, total suspended solids; POM, particulate organic matter; PIM, particulate inorganic matter; OMR, organic matter ratio. The values represent single sampling dates.

Turbidity, TSS, and POM exhibited significant main effects of period ($p < 0.05$), with substantially higher values observed during the mucilage period and subsequent declines during the post-mucilage period. A significant station effect was also detected ($p < 0.05$), with stations M1 and M2 recording higher turbidity, TSS, and POM than station R during May; however, these spatial differences were absent in October, when values at all three stations converged to comparably low levels. This pattern, pronounced inter-station differences in May but not in October, produced a significant Period × Station interaction ($p < 0.05$), indicating that the effect of station on these variables was period-dependent rather than consistent across sampling occasions. Particulate inorganic matter was significantly affected by period ($p < 0.05$), decreasing markedly from May to October, with neither station nor interaction effects reaching significance ($p > 0.05$). The POM ratio also decreased from the mucilage to the post-mucilage period, reflecting a reduced contribution of organic material to total suspended particulates in October.

Microscopic examination of phytoplankton samples collected in May and October 2025 revealed distinct spatial and temporal differences among the stations. A total of 77 phytoplankton taxa belonging to Dinophyceae, Bacillariophyceae, Euglenophyceae, Cyanophyceae, and Coccolithophyceae were identified across both sampling periods and stations, encompassing phytoplankton associated with amnesic shellfish poisoning (ASP), diarrhetic shellfish poisoning (DSP), mucilage-forming (MU), toxic (T), and non-toxic blooming (NT) groups.

In May, the assemblage was characterized by the co-occurrence of MU and NT taxa at both stations, along with the presence of ASP- and DSP-producing species. Notably, DSP-associated dinoflagellates, including *Dinophysis acuminata*, *Dinophysis caudata*, *Lingulaulax polyedra* (=*Lingulodinium polyedra*), and *Protoperidinium abei var. rotundatum* (=*Peridinium rotundatum*) were recorded primarily in May, indicating an elevated potential for diarrhetic shellfish poisoning during the mucilage phenomenon. ASP-producing diatoms *Pseudo-nitzschia delicatissima* and *Pseudo-nitzschia pungens* were also detected at stations M1 and M2 in May, together with the benthic dinoflagellate *Prorocentrum lima*, further highlighting the coexistence of multiple harmful algal groups during this period.

Mucilage-forming species including *Noctiluca scintillans* (=*Noctiluca miliaris*), *Gonyaulax fragilis*, *Prorocentrum micans Ehrenberg*, *Skeletonema costatum*, *Cylindrotheca closterium*, *Thalassiosira gravida* (=*Thalassiosira rotula*), and *Phaeocystis pouchetii* were widely distributed across both stations in May, often occurring simultaneously with NT taxa, suggesting that mucilage events were supported by a mixed assemblage rather than a single dominant

species. Spatially, both stations exhibited broadly similar functional composition in May; however, station M2 showed slightly higher diversity of DSP and MU taxa, including repeated detections of *Dinophysis* spp. and mucilage-associated dinoflagellates. The dinoflagellate species representing the May period in terms of abundance were *N. scintillans* (72 cells L^{-1}) and *P. micans* (72 cells L^{-1}); the diatom species were *Chaetoceros radiatus* (2080 cells L^{-1}), *Cylindrotheca closterium* (144 cells L^{-1}), *P. delicatissima* (96 cells L^{-1}), and *T. rotula* (336 cells L^{-1}); and the coccolithophore was *P. pouchetii* (400 cells L^{-1}).

In contrast, October (post-mucilage) samples exhibited a marked reduction in harmful functional groups. DSP taxa were largely absent, while ASP-producing *Pseudo-nitzschia pungens* persisted at M1 but was reduced overall. MU taxa remained present but with fewer representatives, primarily *Cylindrotheca closterium* and *Thalassiosira gravida*, indicating a substantial decline in mucilage-associated diversity relative to May. The phytoplankton community during October was dominated by NT species at both stations, particularly centric and pennate diatoms (*Chaetoceros* sp., *Thalassiosira* sp., *Thalassionema* sp., *Tripos* sp.), reflecting a transition toward a non-harmful, bloom-forming assemblage.

The toxic cyanobacterium *Leptolyngbya lagerheimii* was detected exclusively during October at both stations, representing the only T-class taxa recorded in the study. Overall, temporal variation outweighed spatial differences between M1 and M2, as both stations exhibited comparable functional group compositions across each period. The mucilage period was characterized by the simultaneous presence of ASP, DSP, MU, and NT taxa, whereas the recovery period was dominated by NT species with reduced MU representation and near-complete disappearance of DSP taxa, demonstrating a clear seasonal restructuring of the phytoplankton community (Table S1).

Biometric data of the sample groups revealed significant temporal variations in shell dimensions between the mucilage-impacted period (May 2025) and the post-mucilage period (October 2025) (Table 2). During the mucilage event, no significant differences were observed between the mussel groups M1MUS and M2MUS in terms of total shell length (TL), total shell width (TW), and total shell height (TH). Both groups had mean TL values of 31.75 ± 8.55 mm and 29.83 ± 10.56 mm, respectively. Following the recovery period, a significant increase (Kruskal–Wallis, H = 68.65, df = 3, $p < 0.001$) was recorded across all dimensional parameters of the samples in October 2025. The recovery groups (M1REC and M2REC) formed a statistically distinct homogeneous group, with TL increasing to 40.99 ± 3.94 mm and 43.39 ± 3.71 mm, respectively.

Table 2. Morphometric characteristics, dry biomass, and condition index of *Mytilus galloprovincialis* sampled from stations M1 and M2 during the mucilage event in May 2025 (groups M1MUS and M2MUS) and post-mucilage in October 2025 (groups M1REC and M2REC) in the Gulf of Erdek (Marmara Sea). Values are expressed as mean ± standard deviation. Statistically significant differences between groups ($p < 0.05$) are indicated by different superscript letters within each column.

Period	Groups	TL (mm)	TW (mm)	TH (mm)	Dry Shell (g)	Dry Meat (g)	CI
May 2025	M1MUS	31.75 ± 8.55 ^{a}	15.90 ± 4.22 ^{a}	10.66 ± 2.45 ^{a}	2.39 ± 1.23 ^{b}	0.09 ± 0.06 ^{a}	3.69 ± 0.79 ^{a}
	M2MUS	29.83 ± 10.56 ^{a}	14.87 ± 4.95 ^{a}	9.64 ± 3.13 ^{a}	1.27 ± 0.89 ^{a}	0.05 ± 0.03 ^{b}	3.70 ± 0.99 ^{a}
October 2025	M1REC	40.99 ± 3.94 ^{b}	20.86 ± 2.11 ^{b}	14.36 ± 1.65 ^{b}	2.08 ± 0.55 ^{bc}	0.12 ± 0.04 ^{c}	6.03 ± 1.54 ^{b}
	M2REC	43.39 ± 3.71 ^{b}	22.48 ± 2.34 ^{b}	15.49 ± 1.48 ^{b}	2.50 ± 0.62 ^{c}	0.15 ± 0.04 ^{c}	6.04 ± 1.30 ^{b}

TL, total shell length; TW, total shell width; TH, total shell height; CI, condition index.

Dry shell and dry meat weights exhibited distinct patterns of variation (Table 2). In May, dry shell weight varied significantly between groups (Kruskal–Wallis, H = 54.06, df = 3, $p < 0.001$); M2MUS recorded the lowest mean value at 1.27 ± 0.89 g, which was significantly lower than the mean value for M1MUS (2.39 ± 1.23 g). In October, dry shell weights stabilized, with M2REC reaching the highest recorded mean values at 2.50 ± 0.62 g.

The impact of mucilage events on dry meat yield was heterogeneous, with station-dependent differences observed between aquaculture sites during the event period. In May, the M2MUS group exhibited significantly lower mean meat biomass (0.05 ± 0.03 g) than the M1MUS group (0.09 ± 0.06 g) (Kruskal–Wallis, H = 96.85, df = 3, $p = 0.000$). However, during the post-mucilage period in October 2025, both groups sampled from mussel farm stations exhibited compensatory growth, forming a statistically higher group ($p < 0.05$) with dry meat weights increasing to 0.12 ± 0.04 g (M1REC) and 0.15 ± 0.04 g (M2REC).

The Kruskal–Wallis test revealed a distinct separation between sampling periods for CI, irrespective of the station (Table 2). Mean CI values were critically low; however, no significant difference was observed between M1MUS (3.69 ± 0.79) and M2MUS (3.70 ± 0.99) during the mucilage event in May 2025 (Kruskal–Wallis, H = 110.27, df = 3, $p > 0.05$). However, the mean CI values of the M1REC and M2REC groups significantly increased ($p < 0.001$) by approximately 63%, reaching 6.03 ± 1.54 and 6.04 ± 1.30, respectively (Figure 3).

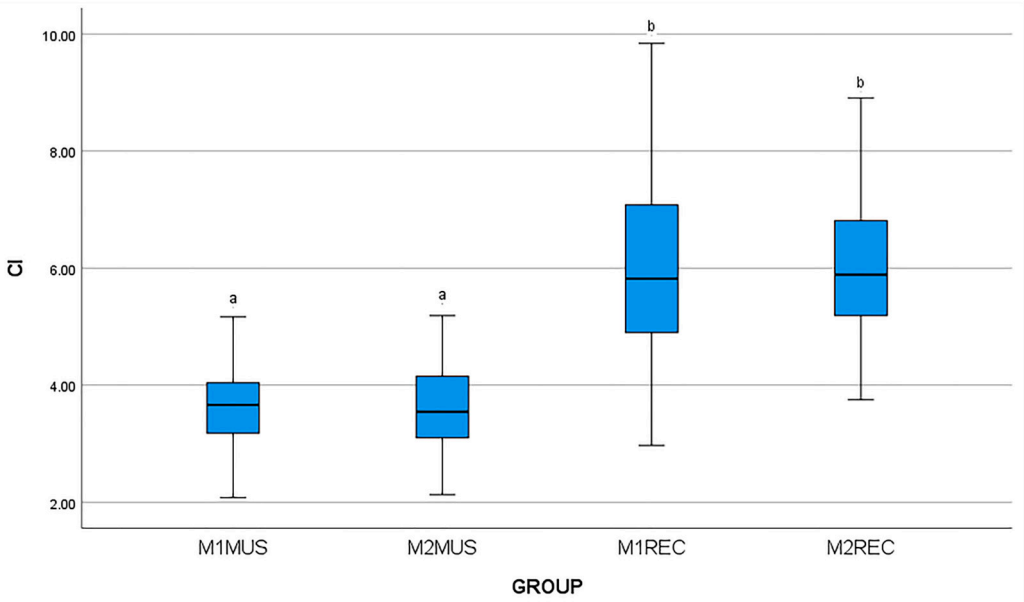

Figure 3. Condition index (CI) of *Mytilus galloprovincialis* sampled (n = 200) from longlines of a mussel aquaculture farm in the Gulf of Erdek (Marmara Sea) during the mucilage event in May 2025 (Groups M1MUS and M2MUS) and during the post-mucilage period in October 2025 (Groups M1REC and M2REC). Different superscripts indicate significant differences at $p < 0.05$. The error bars indicating the standard deviation.

4. Discussion

The results of this study provide evidence that the 2025 mucilage event in the Gulf of Erdek imposed measurable environmental stress on mussel aquaculture conditions, with sampling period accounting for a substantially greater proportion of variance in most water quality parameters than station in the two-way ANOVA. This pattern is consistent with our second hypothesis, that water quality deterioration during mucilage, specifically hypoxia and elevated organic loading, mediates effects on mussel physiology, and suggests that temporal forcing associated with contrasting mucilage and post-mucilage conditions was the dominant source of variability captured by the study design. However, this interpretation requires qualification. Significant station effects were detected for dissolved oxygen, pH, turbidity, TSS, and POM, particularly during May 2025, with coastal aquaculture stations M1 and M2 consistently recording more degraded conditions than the offshore reference station R. The significant Period × Station interaction for turbidity, TSS, and POM further confirms that spatial differences were not negligible but were period-dependent, being pronounced during the mucilage event and absent during post-mucilage recovery.

Taken together, the data support a characterization of predominantly temporal but spatially modulated stress, rather than purely temporal stress as initially stated.

It must also be acknowledged that the two-station aquaculture design, with M1 and M2 separated by approximately 17 km along a north–south transect, was not designed to detect fine-scale spatial heterogeneity within the gulf. Localized phenomena such as hypoxic micropatches, nearshore accumulation gradients driven by current asymmetries, or farm-scale hydrodynamic effects on mucilage retention could plausibly have generated spatial variability at scales smaller than the inter-station distance, which would have remained undetected in the present design. The convergence of biometric and condition index responses between M1 and M2 during both periods, supporting our first hypothesis of uniform mucilage-induced growth suppression, may therefore partly reflect the limited spatial resolution of the design rather than true spatial homogeneity of impact across the gulf.

Furthermore, with sampling conducted at only two discrete time points, one during the active mucilage event in May and one five months later in October, the study was not designed to resolve the onset, peak intensity, or decay trajectory of the mucilage event, nor the intermediate physiological dynamics of mussels during the transition between periods. The five-month interval between sampling occasions means that the observed recovery in shell dimensions, dry biomass, and condition index reflects the net outcome of a prolonged and variable post-event period rather than a temporally resolved recovery trajectory. Consequently, while the contrast between periods provides a clear signal reflected in biometric indicators consistent with mucilage-associated growth impairment and subsequent recovery, supporting hypotheses (i) and (ii), it is insufficient to draw definitive mechanistic conclusions regarding the duration, intensity, or cumulative physiological cost of the 2025 mucilage event. Future studies should incorporate higher-frequency, multi-station sampling across varying distances from shore and across multiple seasons to resolve both the fine-scale spatial heterogeneity and the temporal dynamics of mucilage impacts on mussel aquaculture in this system.

The recurrent mucilage outbreaks in the Gulf of Erdek reflect the convergence of multiple interacting environmental drivers. As a semi-enclosed embayment with restricted water exchange and long residence times [4], the gulf retains nutrient-enriched water masses that, combined with agricultural and terrestrial runoff [6], sustain the eutrophic conditions favorable to EPS overproduction by mucilage-forming phytoplankton [73]. Pronounced seasonal stratification further suppresses vertical mixing and promotes extracellular polysaccharide release under nutrient-depleted, light-saturated conditions [1,23]. The shallow bathymetry of the coastal zones facilitates benthic mucilage retention, as evidenced by persistent seabed accumulations documented throughout 2023 and 2024 [74], while basin-scale transport via the two-layer Marmara circulation introduces additional organic aggregates and EPS-producing taxa from the broader sea. Rising sea surface temperatures are intensifying and prolonging stratification, amplifying the frequency and persistence of outbreaks, consistent with the irregular mucilage recurrence in the gulf from 2021 through 2025 [10].

Measurements of DO in heavily affected coastal areas during the 2021 Marmara Sea mucilage phenomenon showed DO levels plunging to lethal ranges of 2.4–4.6 mg L^{-1}, directly resulting in the mass mortality of fish, sponges, and corals [75]. The determined DO levels as low as 3.1 to 4.4 mg L^{-1} during the mucilage event in May 2025 coincide with the findings of relevant studies in literature which reported the rapid depletion of oxygen levels as the most severe impact [1,14,75–77]. Such levels may not have a lethal effect in the short term, as *M. galloprovincialis* has been reported to adapt to depleted DO conditions of 2.2–2.75 mg L^{-1} without mortality [78,79]; however, suppression of the immune response and increased oxidative stress are the primary sublethal effects that ultimately

inhibit growth [80]. Yümün and Kam [81], reported that mucilage itself was an acidic aggregate whose pH level is as low as 6.4 itself and 7.13 to 7.25 in the mucilage impacted seawater. The observed mean pH levels of 6.85 at mussel aquaculture stations and 6.92 at the reference station during May 2025 in this study reflect the combined impact of hypoxic conditions on seawater acidification during mucilage events, as reported in several studies on water quality affected by mucilage [75,82,83]. The pH level significantly increased to a mean of 7.66 in the post-mucilage period (October 2025), close to the standard of the Marmara Sea [75,84]; however, several studies have reported wide-ranging negative effects of acidification on Mediterranean mussels across multiple biological levels, including shell integrity, physiology, larval development, immunity, and attachment [85–89]. Similarly, low meat yield efficiency, decreased growth, and reduced ability to attach to cultivation ropes are also among the most significant observations of this study.

The microscopic identification of DSP-producing dinoflagellates including *D. acuminata*, *D. caudata*, and *L. polyedra*, as well as ASP-producing diatoms *P. delicatissima* and *P. pungens*, at both aquaculture stations during May 2025 indicates that mussel farms were situated within a phytoplankton community structure carrying an elevated potential toxicity risk during the mucilage period. The simultaneous presence of these taxa within a mucilage-dominated assemblage reflects the convergence of thermal stratification, elevated organic loading, and nutrient enrichment that characterize the gulf during late spring: stratification-driven nutrient depletion selectively favors motile dinoflagellates capable of vertical migration, while dissolved organic matter accumulation within the EPS matrix sustains mixotrophic Dinophysis nutrition through proliferating ciliate prey, and the EPS matrix itself reduces turbulent diffusion, prolonging HAB cell residence times and amplifying local cell densities beyond growth-rate predictions alone [6,90,91]. Similar coupling of mucilage formation and HAB intensification under comparable stratification and eutrophication forcing has been reported from the northern Adriatic [21,22], the Gulf of Lion [92], and the northern Aegean Sea [36], suggesting that the Gulf of Erdek conforms to a broader regional pattern of mucilage-HAB co-occurrence in eastern Mediterranean semi-enclosed basins. It must nonetheless be explicitly acknowledged that no toxin analyses of mussel tissues or water samples were conducted in this study, and the identification of toxigenic taxa by microscopy alone cannot confirm active toxin production or tissue accumulation. The co-occurrence of HAB-associated and mucilage-forming taxa therefore represents an elevated risk condition rather than a confirmed toxicological hazard, and should be interpreted as a precautionary inference based on community composition rather than direct toxicological evidence [92,93].

The shift toward communities dominated by non-toxic bloomers during the post-mucilage period suggests that mussel farms rapidly transitioned back to more typical seasonal phytoplankton conditions, which is broadly consistent with documented patterns of phytoplankton succession. Research on HAB dynamics in coastal systems confirms that non-toxic bloom-forming species tend to dominate in the aftermath of major disturbance events, as environmental conditions shift away from those favoring the original bloom taxa [25]. Monitoring programs in Scottish waters have similarly shown that the dominance of particular HAB genera is temporally constrained, with communities reorganizing along seasonal gradients [94]. However, the appearance of the toxic cyanobacterium *L. lagerheimii* in October indicates that recovery phases may still harbor emerging or secondary hazards distinct from those present during the peak mucilage event. The studies on cyanobacterial toxin producers highlights that species such as those producing microcystins, nodularins, and saxitoxins can emerge under conditions that differ markedly from those favoring classical HAB taxa [95,96]. Moreover, toxic phytoplankton can persist in subsurface thin layers or at low concentrations undetectable by conventional monitoring, yet still transfer

toxins to higher trophic levels, including shellfish [97]. The accumulation of cyanobacterial toxins in bivalves, including mussels (*Mytilus edulis*), has also been experimentally confirmed, establishing a direct pathway for toxin transfer to aquaculture products [98–101]. This highlights that post-event conditions should not be assumed safe solely based on the disappearance of classical HAB taxa; rather, mussel aquaculture requires extended post-disturbance surveillance to capture delayed or seasonally shifting toxicity risks. The economic consequences of inadequate surveillance are substantial, with HAB-associated biotoxins causing significant annual losses in mussel production [94,102].

Notably, the elevated diversity and abundance of phytoplankton, particularly MU and HAB taxa, observed in May likely resulted from high DOM concentrations produced during mucilage-associated bacterial enzymatic degradation, as demonstrated by Olson et al. [103]. Such conditions amplify the selective advantage of taxa capable of exploiting enriched organic substrates, which may, in turn, intensify the severity of mucilage impacts on filter feeders. For mussels, the combination of high particulate loads (TSS, POM), depressed oxygen, lowered pH, and HAB presence creates a cumulative stress environment that can explain the suppressed growth and reduced condition indices recorded during the event. These findings align with earlier work indicating that mussels under simultaneous hypoxic and toxic stress exhibit reduced feeding efficiency [104], impaired metabolic activity [105], and weakened physiological resilience [106,107].

Shell dimensions (TL, TW, and TH) displayed clear temporal separation between the mucilage event and the post-mucilage period. During May sampling, both stations exhibited comparably low mean values, indicating suppression-consistent patterns of shell growth regardless of spatial differences. The absence of significant differences between M1MUS and M2MUS suggests that the mucilage phenomenon imposed a uniform limitation on growth, likely through reduced feeding efficiency and high particulate loads interfering with valve activity. By October 2025, a significant increase in shell dimensions reflected the resumption of normal somatic growth. The lack of differences between M1REC and M2REC indicates homogeneous recovery across the gulf, implying that the environmental conditions supporting post-mucilage growth, such as improved water clarity, increased phytoplankton availability, and normalized oxygen levels, were widespread in the aquaculture area. The pronounced increase in total shell length across both post-mucilage groups underscores the species' capacity for rapid shell growth once environmental stressors are alleviated. Peharda et al. [108] and Yıldız et al. [109] provided converging evidence that mussels increase condition and logic for growth during favorable periods or post-stress, consistent with rapid shell growth in the post-mucilage phase.

Dry shell and dry meat weights exhibited a more complex pattern than shell dimensions, showing station-dependent differences during the mucilage event. In particular, the M2MUS group exhibited significantly lower shell and meat biomass than the M1MUS group. This suggests that, despite the absence of statistically significant differences in TSS, POM, turbidity, and OMR among stations, the relatively higher values of these parameters at the M2 station exerted a stronger adverse effect on mussels. In contrast, the October samples revealed a clear compensatory response in both dry shell and dry meat weights, especially in M2REC, which reached the highest mean shell and meat biomasses among all groups. This compensation suggests that individuals experiencing greater biomass loss during the mucilage event may have accelerated their feeding and growth rates once conditions improved. Such compensatory mechanisms are well documented in cultivated bivalves exposed to episodic stress, in which rapid rebuilding of tissue mass occurs upon restoration of favorable environmental conditions [110,111].

Among all the measured parameters, CI was the most sensitive indicator of physiological impairment. The critically low CI values observed in May compared to the historical

data from the region indicated a substantial reduction in the energy reserves and overall health of mussels during the mucilage event. The similarity between M1MUS and M2MUS suggests that both stations were equally subjected to mucilage-induced stress, although their biomass responses differed. The CI values between 3.69 and 3.70 during the mucilage event in late spring in this study were lower than the values of 5.94–7.30 reported by Acarlı et al. [112] for wild samples collected from south of the Marmara Sea. Moreover, one of the limited studies on the growth of cultured mussels in the Marmara Sea, reported a top CI value of 17.91 in May 2019 [113] that is significantly different from the growth parameters in this study. Contrary to our findings, authors indicated that months April, May and June are the optimal periods for harvest of mussels when the CI is at its maximum point. Similarly, Yildirim et al. [114] reported a meat yield of 23% in May for Mediterranean mussels in an aquaculture farm located in Gulf of Erdek, close to the M2 station in our study. The mean CI of 6.04 recorded in October 2025 was also significantly below the 10.56 and 17.43 CI values of Acarli, Vural and Yildiz [113] and Yildirim, Erdem, Sabanci, Gökvardar, Serdar and Ertan [114] for the month of October 2019 and 2016, respectively. CI value of October 2025 in this study that is approximately 63% higher than May indicates a substantial physiological recovery driven by improved environmental conditions, however such lowest value among the historical data shows the residual effects of mucilage stress persisted throughout the growth period after the mucilage event. In contrast, the absence of mucilage-free aquaculture sites in the Gulf of Erdek and nearby areas precluded the inclusion of a control group of mussels to isolate the sole effects of mucilage on growth patterns in this study. Therefore, future research incorporating a control group from mucilage-free aquaculture sites would strengthen and more reliably determine the comparative impact of mucilage on mussel growth.

Finally, although this study documented clear temporal links between phytoplankton community composition, mucilage formation, and mussel growth performance, the absence of long-term and multi-seasonal sampling limits the ability to resolve the mechanistic pathways through which mucilage events propagate ecological and aquaculture impacts [34,115]. Future studies should (i) conduct multi-seasonal monitoring to capture interannual variability in mucilage intensity and its delayed physiological effects; (ii) integrate biochemical and molecular biomarkers to better identify sublethal stress responses; and (iii) evaluate food availability and seston composition with higher temporal resolution to refine cause–effect relationships.

5. Conclusions

The results collectively show that mucilage events pose a serious but reversible threat to mussel aquaculture. While the mucilage outbreak period was associated with markedly reduced biometric indices and depleted biomass relative to regional historical baselines, the species demonstrated considerable resilience once the stressor subsided. However, the station-specific disparities in biomass reductions observed in May highlight the importance of farm layout, hydrodynamics, and localized environmental gradients in determining the severity of mucilage impacts. For aquaculture management, these findings emphasize the need for spatially explicit monitoring strategies, particularly in regions prone to mucilage formation. Early detection systems, combined with temporary harvesting adjustments or stock relocation, could help mitigate the economic impacts of future events. Moreover, the strong compensatory growth observed indicates that timely post-event environmental improvements can support biomass recovery, suggesting that ecosystem-level restoration efforts may directly benefit farm productivity.

Supplementary Materials: The following supporting information can be downloaded at: https://www.mdpi.com/article/10.3390/d18040238/s1, Table S1. Spatial and temporal distribution of phytoplankton taxa with indication of HAB species at stations M1 and M2 during May 2025 (mucilage event) and October 2025 (post-mucilage period).

Author Contributions: Conceptualization, M.T.T.; methodology, M.T.T. and L.Y.; software, M.T.T. and L.Y.; validation, M.T.T. and L.Y.; formal analysis, M.T.T. and L.Y.; investigation, M.T.T. and L.Y.; resources, M.T.T.; data curation, M.T.T. and L.Y.; writing—original draft preparation, M.T.T. and L.Y.; writing—review and editing, M.T.T. and L.Y.; visualization, M.T.T. and L.Y. All authors have read and agreed to the published version of the manuscript.

Funding: This research received no external funding.

Institutional Review Board Statement: Mussels are not classified as aquatic vertebrate and do not require ethical approval according to international and domestic laws of Türkiye. (https://eusocyek.ege.edu.tr/tr-20671/yonerge.html, accessed on 8 March 2026).

Data Availability Statement: The original contributions presented in this study are included in the article. Further inquiries can be directed to the corresponding author.

Conflicts of Interest: The authors declare no conflicts of interest.

Abbreviations

The following abbreviations are used in this manuscript:

ANOVA	Analysis of variance
ASP	Amnesic Shellfish Poisoning
CI	Condition Index
DO	Dissolved Oxygen
DSP	Diarrhetic Shellfish Poisoning
HAB	Harmful Algal Bloom
MU	Mucilage-forming Species
NT	Non-toxic Blooming Species
OMR	Organic Matter Ratio
PIM	Particulate Inorganic Matter
POM	Particulate Organic Matter
PSP	Paralytic Shellfish Poisoning
T	Toxic Species
TL	Total Shell Length
TH	Total Shell Height
TSS	Total Suspended Solids
TW	Total Shell Width

References

1. Savun-Hekimoğlu, B.; Gazioğlu, C. Mucilage problem in the semi-enclosed seas: Recent outbreak in the Sea of Marmara. *Int. J. Environ. Geoinform.* **2021**, *8*, 402–413. [CrossRef]
2. Della Torre Tassis, L. Notizie sulla vasta fioritura algale (diatomee "cosa moccichiosa") dell'anno 1729. *Racc. D'opus. Sci. Filol. 1746*, 256–257.
3. Innamorati, M.; Melley, A.; Nuccio, C.; Castelli, C.; Balzi, M. Le mucillaggini tirreniche. *Atti Soc. Toscana Sci. Nat. Resid. Pisa. Memorie. Ser. A* **1995**, 293–307.
4. Fanuko, N.; Valčić, M.; Skenderović, J. Relationship Between the Mucilage Phenomenon and Some Concomitant Environmental Variables in the Northern-Adriatic Lagoon of Stella Maris, Umag, Croatia. *Pomor. J. Marit. Stud.* **2008**, *22*, 73–87.
5. Precali, R.; Giani, M.; Marini, M.; Grilli, F.; Ferrari, C.R.; Pečar, O.; Paschini, E. Mucilaginous aggregates in the northern Adriatic in the period 1999–2002: Typology and distribution. *Sci. Total Environ.* **2005**, *353*, 10–23. [CrossRef]
6. Degobbis, D.; Precali, R.; Ferrari, C.R.; Djakovac, T.; Rinaldi, A.; Ivančić, I.; Gismondi, M.; Smodlaka, N. Changes in nutrient concentrations and ratios during mucilage events in the period 1999–2002. *Sci. Total Environ.* **2005**, *353*, 103–114. [CrossRef]

7. Aktan, Y. Mucilage event associated with diatoms and dinoflagellates in Sea of Marmara, Turkey. *Harmful Algae News* **2008**, *36*, 1–3.
8. Tüfekçi, V.; Balkis, N.; Beken, C.P.; Ediger, D.; Mantikci, M. Phytoplankton composition and environmental conditions of the mucilage event in the Sea of Marmara. *Turk. J. Biol.* **2010**, *34*, 199–210. [CrossRef]
9. Yurga, L. Distribution of phytoplanktonic species in the sea snot in 2021 in the Marmara Sea. *Ege J. Fish. Aquat. Sci. (EgeJFAS)/Su Ürünleri Derg.* **2022**, *39*, 235–242. [CrossRef]
10. Sarı, M.; Karadurmuş, U. Documenting the emergence of a new mucilage formation in the Sea of Marmara in 2024. *Turk. J. Marit. Mar. Sci.* **2026**. *Epub ahead of printing*. [CrossRef]
11. TURKSTAT. *Production Quantity of Aquaculture Products*; Fishery Statistics; Turkish Statistical Institute: Ankara, Turkey, 2025.
12. Dindar, E. Assessment of pollution status using Water Quality Index (WQI) and hydrochemical ındicators in the Gemlik Gulf, Marmara Sea, Türkiye: A spatial and temporal perspective. *Environ. Sci. Pollut. Res.* **2025**, *32*, 14860–14890. [CrossRef] [PubMed]
13. Isinibilir, M.; Yüksel, E.; Martell, L.; Topçu, N. No escape from the mucilage impact: Even opportunistic hydroids were affected in the catastrophic mucilage of 2021 in the Sea of Marmara. *Reg. Stud. Mar. Sci.* **2024**, *77*, 103678. [CrossRef]
14. Karadurmuş, U.; Sarı, M. Marine mucilage in the Sea of Marmara and its effects on the marine ecosystem: Mass deaths. *Turk. J. Zool.* **2022**, *46*, 93–102.
15. Yılmaz, E.; Harmantepe, F.B. Aquaculture in Çanakkale: Current Status and Future Perspectives. *MEMBA Bilim. Derg.* **2025**, *11*, 116–129. [CrossRef]
16. Dzierżyńska-Białończyk, A.; Jermacz, Ł.; Zielska, J.; Kobak, J. What scares a mussel? Changes in valve movement pattern as an immediate response of a byssate bivalve to biotic factors. *Hydrobiologia* **2019**, *841*, 65–77. [CrossRef]
17. Koncagül, M.; Dülger, N.E.; Yinanç, A. Dünyada ve Marmara Denizi'nde müsilaj oluşumu ve etkileri. *Eur. J. Eng. Appl. Sci.* **2022**, *5*, 73–79. [CrossRef]
18. Rinaldi, A.; Vollenweider, R.; Montanari, G.; Ferrari, C.; Ghetti, A. Mucilages in Italian seas: The Adriatic and Tyrrhenian seas, 1988–1991. *Sci. Total Environ.* **1995**, *165*, 165–183. [CrossRef]
19. Cornello, M.; Boscolo, R.; Giovanardi, O. Do mucous aggregates affect macro-zoobenthic community and mussel culture? A study in a coastal area of the Northwestern Adriatic Sea. *Sci. Total Environ.* **2005**, *353*, 329–339. [CrossRef]
20. Han, L.; Zhang, J.; Lang, C.; Li, W.; Wu, Z.; He, X.; Wang, X.; Yu, J.; Li, Q.; Li, Y. Mussel culture activities facilitate the export and burial of particulate organic carbon. *J. Mar. Sci. Eng.* **2024**, *12*, 910. [CrossRef]
21. Pierre, C.; Vallet, G. A mathematical model of marine mucilage, the case of the liga on the Basque coast. *Math. Model. Nat. Phenom.* **2023**, *18*, 34. [CrossRef]
22. Totti, C.; Cangini, M.; Ferrari, C.; Kraus, R.; Pompei, M.; Pugnetti, A.; Romagnoli, T.; Vanucci, S.; Socal, G. Phytoplankton size-distribution and community structure in relation to mucilage occurrence in the northern Adriatic Sea. *Sci. Total Environ.* **2005**, *353*, 204–217. [CrossRef] [PubMed]
23. Danovaro, R.; Umani, S.F.; Pusceddu, A. Climate change and the potential spreading of marine mucilage and microbial pathogens in the Mediterranean Sea. *PLoS ONE* **2009**, *4*, e7006. [CrossRef]
24. Vilibić, I.; Terzić, E.; Vrdoljak, I.; Novković, I.D.; Vodopivec, M.; Ciglenečki, I.; Djakovac, T.; Hamer, B. Extraordinary mucilage event in the northern Adriatic in 2024—A glimpse into the future climate? *Estuar. Coast. Shelf Sci.* **2025**, *317*, 109222. [CrossRef]
25. Ruvindy, R.; Ajani, P.A.; Ashlin, S.; Hallegraeff, G.; Klemm, K.; Bolch, C.J.; Ugalde, S.; Van Asten, M.; Woodcock, S.; Tesoriero, M. An on-farm workflow for predictive management of Paralytic Shellfish Toxin-producing harmful algal blooms for the aquaculture industry. *Environ. Sci. Technol.* **2024**, *58*, 6924–6933. [CrossRef]
26. Karakulak, F.S.; Kahraman, A.E.; Uzer, U.; Gül, B.; Doğu, S. Effects of mucilage on the fisheries in the Sea of Marmara. *M. Albay Mucilage Probl. Sea Marmara* **2023**, 193–215. [CrossRef]
27. Keleş, G.; Yılmaz, S.; Zengin, M. Possible economic effects of musilage on Sea of Marmara fisheries. *Int. J. Agric. For. Life Sci.* **2020**, *4*, 173–177.
28. Boalch, G.; Harbour, D. Unusual diatom off the coast of south-west England and its effect on fishing. *Nature* **1977**, *269*, 687–688. [CrossRef]
29. Schiaparelli, S.; Castellano, M.; Povero, P.; Sartoni, G.; Cattaneo-Vietti, R. A benthic mucilage event in North-Western Mediterranean Sea and its possible relationships with the summer 2003 European heatwave: Short term effects on littoral rocky assemblages. *Mar. Ecol.* **2007**, *28*, 341–353. [CrossRef]
30. Uflaz, E.; Akyüz, E.; Bolat, F.; Bolat, P.; Arslan, Ö. Investigation of the effects of mucilage on maritime operation. *J. Black Sea/Mediterr. Environ.* **2021**, *27*, 140–153.
31. Üçok, D.; Tosun, Ş.Y.; Erkan, N.; Can Tunçelli, İ.; Doğruyol, H.; Ulusoy, Ş.; Mol, S.; Özden, Ö.; Dagsuyu, E.; Yanardag, R. Microbial seafood safety assessment following a marine mucilage disaster in the Sea of Marmara. *Environ. Microbiol. Rep.* **2025**, *17*, e70050. [CrossRef] [PubMed]
32. Lancelot, C. The mucilage phenomenon in the continental coastal waters of the North Sea. *Sci. Total Environ.* **1995**, *165*, 83–102. [CrossRef]
33. Bradstock, M.; MacKenzie, L. The Tasman Bay Slime Story. *Catch* **1981**, *81*, 29–30.
34. Vollenweider, R.; Montanari, G.; Rinaldi, A. Statistical inferences about the mucilage events in the Adriatic Sea, with special reference to recurrence patterns and claimed relationship to sun activity cycles. *Sci. Total Environ.* **1995**, *165*, 213–224. [CrossRef]

35. Melley, A.; Innamorati, M.; Nuccio, C.; Piccardi, R.; Benelli, M. Caratterizzazione e stagionalitadelle mucillaggini tirreniche. *Biol. Mar. Mediterr.* **1998**, *5*, 203–213.
36. Nikolaidis, G.; Aligizaki, K.; Koukaras, K.; Moschandreou, K. Mucilage phenomena in North Aegean Sea, Greece: Another harmful effect of dinoflagellates. In Proceedings of the 12th International Conference on Harmful Algae, Copenhagen, Denmark, 4–8 September 2006; pp. 4–8.
37. Parsons, T.; Maita, Y.; Lalli, C.M. Amanual of chemical and biological methods for seawater analysis. *Biol. Oceanogr. Process.* **1984**, *173*. [CrossRef]
38. Utermöhl, H. Zur vervollkommnung der quantitativen phytoplankton-methodik: Mit 1 Tabelle und 15 abbildungen im Text und auf 1 Tafel. *Int. Ver. Theor. Angew. Limnol. Mitteilungen* **1958**, *9*, 1–38. [CrossRef]
39. Lackey, J.B. The manipulation and counting of river plankton and changes in some organisms due to formalin preservation. *Public Health Rep. (1896–1970)* **1938**, *53*, 2080–2093. [CrossRef]
40. Anderson, D.M. Toxic red tides and harmful algal blooms: A practical challenge in coastal oceanography. *Rev. Geophys.* **1995**, *33*, 1189–1200. [CrossRef]
41. Balech, E. Los Dinoflagelados del Atlantico sudoccidental. *Publ. Espec. Inst. Esp. Oceanogr.* **1988**, *1*, 1–310.
42. Cupp, E. Marine plankton diatoms of the wast coast of north America. *Scripps Inst. Oceanogr. Univ. Calif. Bull.* **1943**, *5*, 1–238.
43. Delgado, M.; Fortuño, J.M. Atlas de Fitoplancton del Mar Mediterráneo. *Sci. Mar.* **1991**, *55*, 1–130.
44. Dodge, J.D.; Hart-Jones, B. *Marine dinoflagellates of the British Isles*; H.M. Stationery Office: Ann Arbor, MI, USA, 1982.
45. Hasle, G.R.; Syvertsen, E.E. *Chapter 2—Marine Diatoms*; Academic Press: San Diego, CA, USA, 1996.
46. Hendey, N.I. *An Introductory Account of the Smaller Algae of British Coastal Waters: V. Bacillariophyceae (Diatoms)*; HMSO: London, UK, 1964.
47. Koray, T.; Yurga, L.; Çolak-Sabancı, F. *Türkiye Denizleri Mikroplankton (= Protista) Türlerinin Kontrol Listesi ve Tür Tayin Atlası*. Project Report, TÜBİTAK, Grant No: TBAG 102T174: Ankara, Turkey, 2007. Available online: https://search.trdizin.gov.tr/tr/yayin/detay/607813/turkiye-denizleri-mikroplankton-protista-turlerinin-kontrol-listesi-ve-tur-tayin-atlasi (accessed on 10 April 2026).
48. Lebour, M.V. The Planktonic Diatoms of Northern Seas. *Nature* **1930**, *126*, 347. [CrossRef]
49. Marshall, H.G. Phytoplankton Distribution off the North Carolina Coast. *Am. Midl. Nat.* **1969**, *82*, 241–257. [CrossRef]
50. Rampi, L.; Bernhard. *Key for the Determination of Mediterranean Pelagic Diatoms*; CHEN, Dipartimento Radiazioni e Ricerche di Sicurezze e Protezione, Fiascherino: Liguria, Italy, 1978.
51. Rampi, L.; Bernhard, M. *Chiave per la Determinazione delle Peridinee Pelagiche Mediteranee*; Comitato Nazionale Energia Nucleare: Rome, Italy, 1980.
52. Johansen, J.R. Atlas du Phytoplancton Marin Volume II: Diatomophycees. *Phycologia* **1988**, *27*, 431–432. [CrossRef]
53. Steidinger, K.A.; Tangen, K. Dinoflagellates. In *Identifying Marine Diatoms and Dinoflagellates*; Tomas, C.R., Ed.; Academic Press: New York, NY, USA, 1996; pp. 387–598.
54. Steidinger, K.; Williams, J. *Dinoflagellates: Memoirs of the Hourglass Cruises*; Marine Research Laboratory, Florida Department of Natural Resources: St. Petersburg, FL, USA, 1970; Volume 2, p. 1.
55. Sournia, A. Le genre Ceratium (Péridinien Planctonique) dans le canal de Mozambique. Contribution a une révision mondiale première partie. *Vie Milieu* **1967**, 375–440.
56. Sournia, A. *Phytoplankton Manual*; UNESCO: Paris, France, 1978; p. 337.
57. Sournia, A. *Atlas Du Phytoplankton Marine, Volume I. Introduction, Cyanophycées, Dictyochophycées, Dinophycées et Raphidophycées*; Muséum National dHistorie-Naturelle et RCentre National de la Recherche Scientifique, Éditions Du Centre National de La Recherche Scientifique: Paris, France, 1986; p. 15.
58. Taylor, F.J.R. Dinoflagellates from the International Indian Ocean Expedition. A material collected by the RV" Anton Bruun" 1963–1964. *Bibl. Bot.* **1976**, *132*, 1–234.
59. Tomas, C. *Identifying Marine Phytoplankton*; Academic Press: San Diego, CA, USA, 1997; Volume XV.
60. Trégouboff, G.; Rose, M. *Manuel de Planctonologie Mediterranéenne*; Centre National de la Recherche Scientifique: Paris, France, 1957.
61. Wood, E.F. Dinoflagellates in the Australian region. *Mar. Freshw. Res.* **1954**, *5*, 171–352. [CrossRef]
62. Boltovskoy, D. *Atlas del Zooplancton del Atlántico Sudoccidental y Métodos de Trabajo con el Zooplancton Marino*; Publicacion especial del INIDEP: Mar del Plata, Argentina, 1981; p. 936.
63. Isamu, Y. *Illustrations of the Marine Plankton of Japan: Protozoa*, 3rd ed.; Hoikusha Publishing Co., Ltd.: Osaka, Japan, 1982.
64. Lee, J.-B.; Kim, Y.-H. Distribution of tintinnids (loricate ciliates) in East Asian waters in summer. *Coast. Environ. Ecosyst. Issues East China Sea* **2010**, 173–180.
65. Margalef, R. Rôle des ciliés dans le cycle de la vie pélagique en Méditerranée. *Rapp. Procès-Verbaux Réunions Comm. Int. L'exploration Sci. Mer Méditerr.* **1963**, *17*, 463.
66. Pierce, R.W.; Turner, J.T. Global biogeography of marine tintinnids. *Mar. Ecol. Prog. Ser.* **1993**, *94*, 11–26. [CrossRef]
67. AlgaeBase. Listing the World's Algae. Available online: https://www.algaebase.org/ (accessed on 25 November 2025).

68. WoRMS. World Register of Marine Species. Available online: https://www.marinespecies.org/ (accessed on 25 November 2025).
69. Hallegraeff, G.M.; Anderson, D.M.; Cembella, A.D.; Enevoldsen, H.O. *Manual on Harmful Marine Microalgae*; Unesco: Paris, France, 2003; Volume 11.
70. Landsberg, J.H. The effects of harmful algal blooms on aquatic organisms. *Rev. Fish. Sci.* **2002**, *10*, 113–390. [CrossRef]
71. Hurlbert, S.H. Pseudoreplication and the design of ecological field experiments. *Ecol. Monogr.* **1984**, *54*, 187–211. [CrossRef]
72. Crosby, M.P. A review and evaluation of bivalve condition index methodologies with a suggested standard method. *J. Shellfish Res.* **1990**, *9*, 233–237.
73. Polat, E.; Ünver, H.; Altınbaş, M. Müsilaj Oluşumu ve Ekolojisi. *Doğal Afetler Çevre Derg.* **2023**, *9*, 385–403. [CrossRef]
74. Sarı, M.; Karadurmuş, U. Post-mucilage status of the teleost fish assemblages in the Sea of Marmara. *Turk. J. Zool.* **2024**, *48*, 154–164. [CrossRef]
75. Oral, H.V. Environmental statistical analysis on the impacts of marine mucilage on some seawater quality parameters. *Int. J. Environ. Geoinform.* **2023**, *10*, 153–160. [CrossRef]
76. Cozzi, S.; Ivančić, I.; Catalano, G.; Djakovac, T.; Degobbis, D. Dynamics of the oceanographic properties during mucilage appearance in the Northern Adriatic Sea: Analysis of the 1997 event in comparison to earlier events. *J. Mar. Syst.* **2004**, *50*, 223–241. [CrossRef]
77. Misic, C.; Schiaparelli, S.; Harriague, A.C. Organic matter recycling during a mucilage event and its influence on the surrounding environment (Ligurian Sea, NW Mediterranean). *Cont. Shelf Res.* **2011**, *31*, 631–643. [CrossRef]
78. Belivermiş, M.; Kılıç, Ö.; Gezginci-Oktayoglu, S.; Sezer, N.; Demiralp, S.; Şahin, B.; Dupont, S. Physiological and gene expression responses of the mussel *Mytilus galloprovincialis* to low pH and low dissolved oxygen. *Mar. Pollut. Bull.* **2023**, *187*, 114602. [CrossRef] [PubMed]
79. Gostyukhina, O.L.; Kladchenko, E.C.; Chelebieva, E.S.; Tkachuk, A.A.; Lavrichenko, D.S.; Andreyeva, A.Y. Short-Time Salinity Fluctuations Are Strong Activators of Oxidative Stress in Mediterranean Mussel (*Mytilus galloprovincialis*). *Ecol. Montenegrina* **2023**, *63*, 46–58. [CrossRef]
80. Sokolov, E.P.; Adzigbli, L.; Markert, S.; Bundgaard, A.; Fago, A.; Becher, D.; Hirschfeld, C.; Sokolova, I.M. Intrinsic Mechanisms Underlying Hypoxia-Tolerant Mitochondrial Phenotype During Hypoxia-Reoxygenation Stress in a Marine Facultative Anaerobe, the Blue Mussel Mytilus Edulis. *Front. Mar. Sci.* **2021**, *8*, 773734. [CrossRef]
81. Yümün, Z.Ü.; Kam, E. Mucilage Problem and Solution Methods in The Sea of Marmara. In *Ecology of the Marmara Sea: Formation and Interactions of Marine Mucilage, and Recommendations for Solutions*; Muzaffer Şeker, İ.Ö., Ed.; Turkish Academy of Sciences: Ankara, Turkey, 2021; pp. 163–181.
82. Ergul, H.A.; Balkis-Ozdelice, N.; Koral, M.; Aksan, S.; Durmus, T.; Kaya, M.; Kayal, M.; Ekmekci, F.; Canli, O. The early stage of mucilage formation in the Marmara Sea during spring 2021. *J. Black Sea/Mediterr. Environ.* **2021**, *27*, 232–257.
83. Sefercik, U.G.; Colkesen, I.; Kavzoglu, T.; Ozdogan, N.; Ozturk, M.Y. Assessing the physical and chemical characteristics of marine mucilage utilizing in-situ and remote sensing data (Sentinel-1,-2,-3). *PFG–J. Photogramm. Remote Sens. Geoinf. Sci.* **2024**, *92*, 415–430. [CrossRef]
84. Avşar, N.; Aksu, A.; Dinçer, F. Erdek Körfezi (GB Marmara Denizi) bentik foraminifer toplulukları. *Yerbilimleri* **2006**, *27*, 125–141.
85. Bitter, M.C.; Kapsenberg, L.; Gattuso, J.-P.; Pfister, C.A. Standing genetic variation fuels rapid adaptation to ocean acidification. *Nat. Commun.* **2019**, *10*, 5821. [CrossRef]
86. Kapsenberg, L.; Bitter, M.C.; Miglioli, A.; Aparicio-Estalella, C.; Pelejero, C.; Gattuso, J.-P.; Dumollard, R. Molecular basis of ocean acidification sensitivity and adaptation in *Mytilus galloprovincialis*. *iScience* **2022**, *25*, 104677. [CrossRef]
87. Lassoued, J.; Padín, X.; Comeau, L.A.; Bejaoui, N.; Pérez, F.F.; Babarro, J.M. The Mediterranean mussel *Mytilus galloprovincialis*: Responses to climate change scenarios as a function of the original habitat. *Conserv. Physiol.* **2021**, *9*, coaa114. [CrossRef] [PubMed]
88. Lesser, M.P. Climate change stressors cause metabolic depression in the blue mussel, Mytilus edulis, from the Gulf of Maine. *Limnol. Oceanogr.* **2016**, *61*, 1705–1717. [CrossRef]
89. Rahmani, A.; Mathien, C.; Bidault, A.; Le Goïc, N.; Paillard, C.; Pichereau, V. External pH modulation during the growth of Vibrio tapetis, the aetiological agent of brown ring disease. *J. Appl. Microbiol.* **2020**, *129*, 3–16. [CrossRef]
90. Leppard, G.G. The characterization of algal and microbial mucilages and their aggregates in aquatic ecosystems. *Sci. Total Environ.* **1995**, *165*, 103–131. [CrossRef]
91. Umani, S.F.; Ghirardelli, E.; Specchi, M. *Gli Episodi di" Mare Sporco" nell'Adriatico dal 1729 ai Giorni Nostri*; Ufficio Stampa e Pubbliche Relazioni Della Regione Friuli-Venezia Giulia: Trieste, Italy, 1989; p. 178.
92. Tsikoti, C.; Genitsaris, S. Review of harmful algal blooms in the coastal Mediterranean Sea, with a focus on Greek waters. *Diversity* **2021**, *13*, 396. [CrossRef]
93. Fuks, D.; Radić, J.; Radić, T.; Najdek, M.; Blažina, M.; Degobbis, D.; Smodlaka, N. Relationships between heterotrophic bacteria and cyanobacteria in the northern Adriatic in relation to the mucilage phenomenon. *Sci. Total Environ.* **2005**, *353*, 178–188. [CrossRef]
94. Swan, S.; Turner, A.D.; Bresnan, E.; Whyte, C.; Paterson, R.F.; McNeill, S.; Mitchell, E.; Davidson, K. Dinophysis Acuta in Scottish Coastal Waters and Its Influence on Diarrhetic Shellfish Toxin Profiles. *Toxins* **2018**, *10*, 399. [CrossRef]

95. Brito-Echeverría, J.; Pérez, P.A.; Echeveste, P. Assessing environmental drivers of toxin-producing cyanobacteria and phytoplankton in Antarctic and sub-Antarctic waters. *Polar Biol.* **2025**, *48*, 57. [CrossRef]
96. Leal, J.F.; Amado, P.S.M.; Lourenço, J.P.; Cristiano, M.L.S. The Potential of Chitosan-Based Composites for Adsorption of Diarrheic Shellfish Toxins. *Toxins* **2024**, *16*, 200. [CrossRef]
97. Roberts, A.J.; Suttle, C.A. Pathogens and Passengers: Roles for Crustacean Zooplankton Viruses in the Global Ocean. *Microorganisms* **2023**, *11*, 1054. [CrossRef]
98. Buratti, S.; Franzellitti, S.; Poletti, R.; Ceredi, A.; Montanari, G.; Capuzzo, A.; Fabbri, E. Bioaccumulation of algal toxins and changes in physiological parameters in Mediterranean mussels from the North Adriatic Sea (Italy). *Environ. Toxicol.* **2013**, *28*, 451–470. [CrossRef] [PubMed]
99. Chatterjee, S.; More, M. Cyanobacterial Harmful Algal Bloom Toxin Microcystin and Increased Vibrio Occurrence as Climate-Change-Induced Biological Co-Stressors: Exposure and Disease Outcomes via Their Interaction with Gut–Liver–Brain Axis. *Toxins* **2023**, *15*, 289. [CrossRef] [PubMed]
100. Doğruyol, H.; Ulusoy, Ş.; Erkan, N.; Mol, S.; Özden, Ö.; Tuncelli, I.C.; Tosun, Ş.Y.; Üçok, D.; Dağsuyu, E.; Yanardağ, R. Evaluation of biotoxins and toxic metal risks in mussels from the Sea of Marmara following marine mucilage. *Food Chem. Toxicol.* **2024**, *186*, 114558. [CrossRef] [PubMed]
101. Lawrence, J.; Loreal, H.; Toyofuku, H.; Hess, P.; Iddya, K.; Ababouch, L. *Assessment and Management of Biotoxin Risks in Bivalve Molluscs*; FAO Fisheries and Aquaculture Technical Paper; FAO: Rome, Italy, 2011.
102. Chen, K.; Allen, J.D.; Lu, J. Community Structures of Phytoplankton with Emphasis on Toxic Cyanobacteria in an Ohio Inland Lake During Bloom Season. *J. Water Resour. Prot.* **2017**, *9*, 1299–1318. [CrossRef]
103. Olson, N.E.; Cooke, M.E.; Shi, J.H.; Birbeck, J.A.; Westrick, J.A.; Ault, A.P. Harmful Algal Bloom Toxins in Aerosol Generated From Inland Lake Water. *Environ. Sci. Technol.* **2020**, *54*, 4769–4780. [CrossRef] [PubMed]
104. Giacoletti, A.; Sarà, G. Functional spatial contextualisation of the effects of multiple stressors in marine bivalves. *Biosci. Discuss.* **2018**, *2018*, 1–25. [CrossRef]
105. Feidantsis, K.; Giantsis, I.A.; Vratsistas, A.; Makri, S.; Pappa, A.-Z.; Drosopoulou, E.; Anestis, A.; Mavridou, E.; Exadactylos, A.; Vafidis, D.; et al. Correlation Between Intermediary Metabolism, *Hsp* gene Expression, and Oxidative Stress-Related Proteins in Long-Term Thermal-Stressed *Mytilus galloprovincialis*. *Ajp Regul. Integr. Comp. Physiol.* **2020**, *319*, R264–R281. [CrossRef]
106. Freitas, R.; Coppola, F.; Costa, S.; Pretti, C.; Intorre, L.; Meucci, V.; Soares, A.M.V.M.; Solé, M. The Influence of Temperature on the Effects Induced by Triclosan and Diclofenac in Mussels. *Sci. Total Environ.* **2019**, *663*, 992–999. [CrossRef]
107. Fuentes-Santos, I.; Labarta, U.; Fernández-Reiriz, M.J. Characterizing Individual Variability in Mussel (*Mytilus galloprovincialis*) Growth and Testing Its Physiological Drivers Using Functional Data Analysis. *PLoS ONE* **2018**, *13*, e0205981. [CrossRef]
108. Peharda, M.; Župan, I.; Bavčević, L.; Frankić, A.; Klanjšček, T. Growth and Condition Index of Mussel *Mytilus galloprovincialis* in Experimental Integrated Aquaculture. *Aquac. Res.* **2007**, *38*, 1714–1720. [CrossRef]
109. Yıldız, H.; Vural, P.; Acarlı, S. Condition Index, Meat Yield and Biochemical Composition of Mediterranean Mussel (*Mytilus galloprovincialis* Lamarck, 1819) From Canakkale Strait, Turkey. *Alinteri J. Agric. Sci.* **2021**, *36*, 308–314. [CrossRef]
110. Gurr, S.J.; Vadopalas, B.; Roberts, S.B.; Putnam, H.M. Metabolic Recovery and Compensatory Shell Growth of Juvenile Pacific Geoduck *Panopea generosa* Following Short-Term Exposure to Acidified Seawater. *Conserv. Physiol.* **2019**, *8*, coaa024. [CrossRef]
111. Xie, B.; Chen, C.; Zhang, X.; Li, S.; Gu, Z.; Huang, J.; He, J.; Qi, P.; Guo, B.; Liao, Z.; et al. Response of the Metabolic and Autophagy Pathways in Mytilus Under Starvation. *Front. Mar. Sci.* **2022**, *9*, 1014336. [CrossRef]
112. Acarlı, S.; Vural, P.; Yıldız, H. An assessment of the cultivation potential and suitability for human consumption of Mediterranean mussels (*Mytilus galloprovincialis* Lamarck, 1819) from the Yalova coast of the Marmara Sea. *Memba Kastamonu Üniversitesi Ürünleri Fakültesi Derg.* **2023**, *9*, 12–24.
113. Acarli, S.; Vural, P.; Yildiz, H. Temporal variability in biochemical composition and morphometric parameters of cultivated Mediterranean mussels (*Mytilus galloprovincialis*) in Çanakkale, Türkiye. *Reg. Stud. Mar. Sci.* **2024**, *78*, 103759. [CrossRef]
114. Yildirim, Ş.; Erdem, Ö.; Sabanci, F.; Gökvardar, A.; Serdar, S.; Ertan, A. Effects of different culture methods on growth, meat yield, and nutritional composition of Mediterranean mussels (*Mytilus galloprovincialis*), south side of Marmara Sea, Türkiye. *Eur. Zool. J.* **2024**, *91*, 869–889. [CrossRef]
115. Vlašiček, I.; Pfannkuchen, D.M.; Tanković, M.S.; Baričević, A.; Kogovšek, T.; Kužat, N.; Knjaz, M.; Grižančić, L.; Podolšak, I.; Turković, A. High-frequency observations during Adriatic mucilage event reveal unique phytoplankton traits and diversity response. *Sci. Rep.* **2025**, *16*, 1787. [CrossRef] [PubMed]

Disclaimer/Publisher's Note: The statements, opinions and data contained in all publications are solely those of the individual author(s) and contributor(s) and not of MDPI and/or the editor(s). MDPI and/or the editor(s) disclaim responsibility for any injury to people or property resulting from any ideas, methods, instructions or products referred to in the content.